

Mesoporous silicon carbide via nanocasting of Ludox® xerogel

Dmytro Korytko<sup>1</sup>, Svitlana Gryn<sup>1,2</sup>, Sergei Alekseev<sup>1</sup>, Viacheslav Iablokov<sup>3,7</sup>, Olena Khaynakova<sup>4</sup>,  
Vladimir Zaitsev<sup>1,5</sup>, Igor Bezverkhyy<sup>6</sup> and Norbert Kruse<sup>3,7\*</sup>

*1 Taras Shevchenko National University of Kyiv, 64, Volodymyrska Street, 01601 Kyiv, Ukraine*

*2 L.V. Pisarzhevskii Institute of Physical Chemistry NAS of Ukraine, 31 Nauki av, 03028 Kyiv,  
Ukraine*

*3 Université Libre de Bruxelles, Chemical Physics of Materials, Campus Plaine, CP243 Brussels,  
B-1050, Belgium*

*4 Departamento de Química Física y Analítica, Universidad de Oviedo, Julián Clavería 8, Oviedo  
33006, Spain*

*5 Chemistry Department, Pontifical Catholic University of Rio de Janeiro, Rua Marques de São  
Vicente 225, Rio de Janeiro, 22451-900, Brazil*

*6 Laboratoire Interdisciplinaire Carnot de Bourgogne, UMR CNRS 6303, Université de  
Bourgogne, France*

*7 Voiland School of Chemical Engineering and Bioengineering, Washington State University,  
Pullman, Washington 99164, United States*

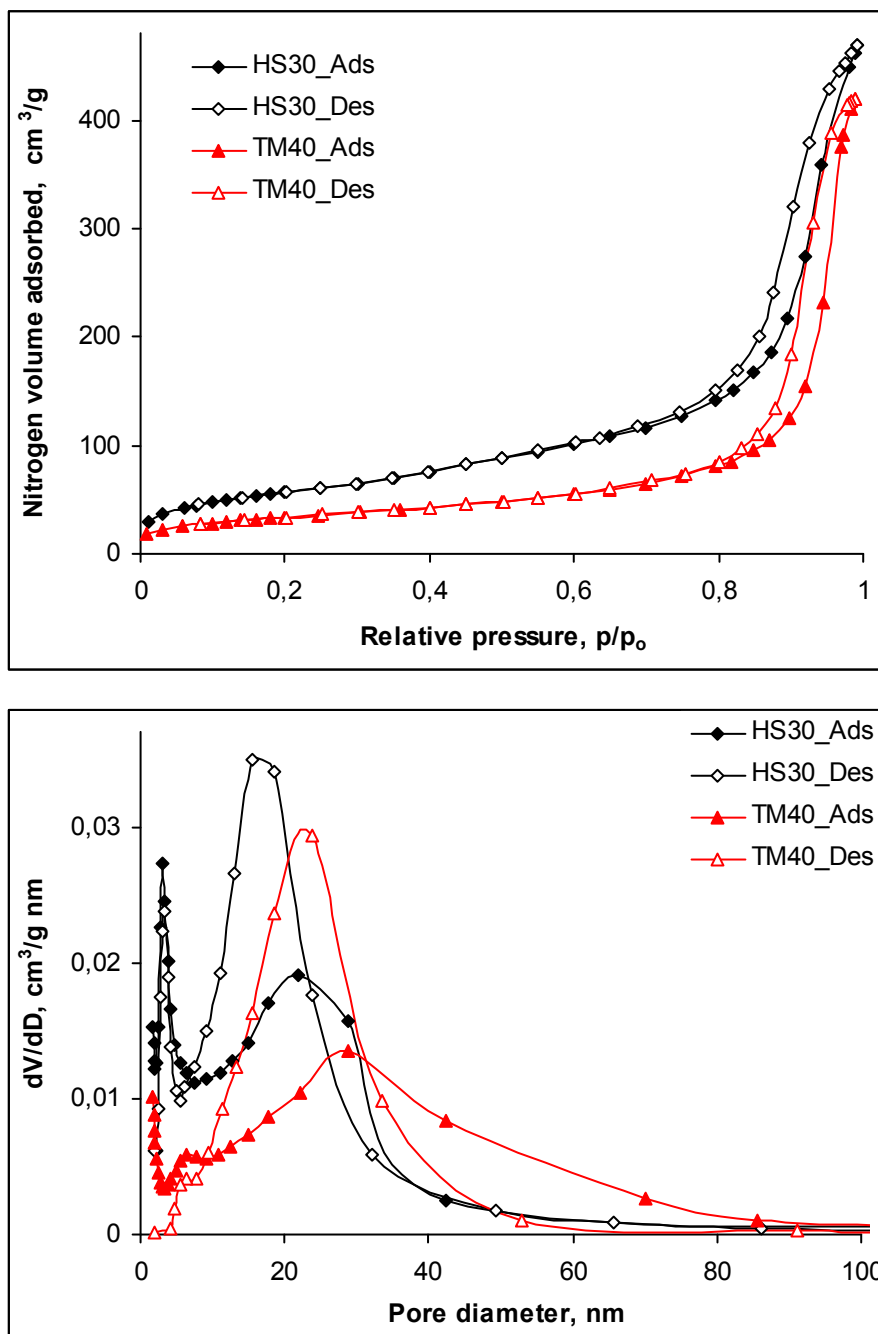
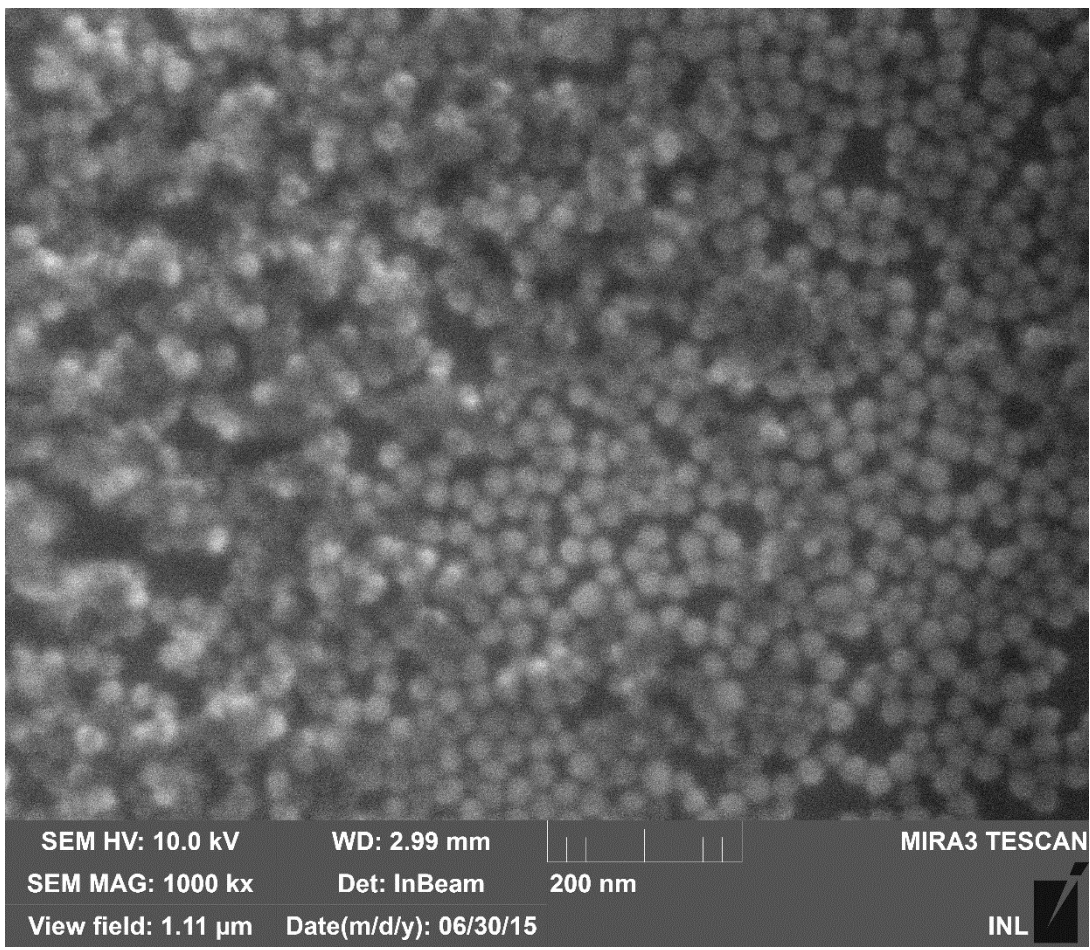


Fig. S1. Nitrogen physisorption isotherms (a) and BJH pore size distributions (b) of Ludox silica xerogels.



SEM HV: 10.0 kV      WD: 2.99 mm  
SEM MAG: 1000 kx      Det: InBeam      200 nm  
View field: 1.11 μm      Date(m/d/y): 06/30/15

MIRA3 TESCAN



Fig. S2. SEM image of Ludox TM40 xerogel.

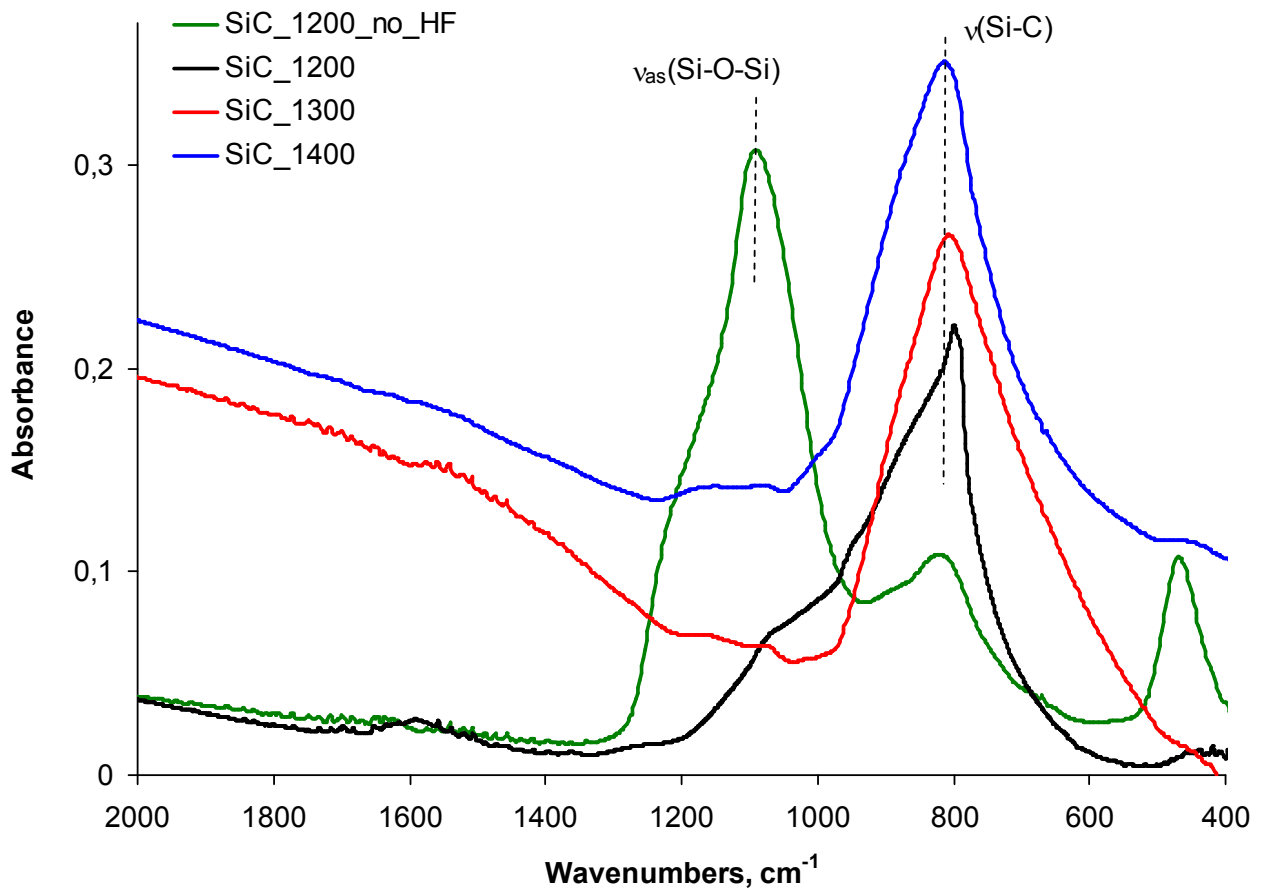


Fig. S3. Absorbance FTIR spectra for the series of SiC-HS-0.6 samples, prepared at different temperatures, before (SiC\_1200\_no\_HF) and after  $\text{SiO}_2$  template leaching.

An intense  $\nu(\text{Si-C})$  band at  $805 \text{ cm}^{-1}$  in the spectra of leached samples is typical for mesoporous SiC; the completeness of the  $\text{SiO}_2$  template removal is confirmed by disappearance of  $\nu(\text{Si-O-Si})$  band at  $1100 \text{ cm}^{-1}$  after HF treatment.

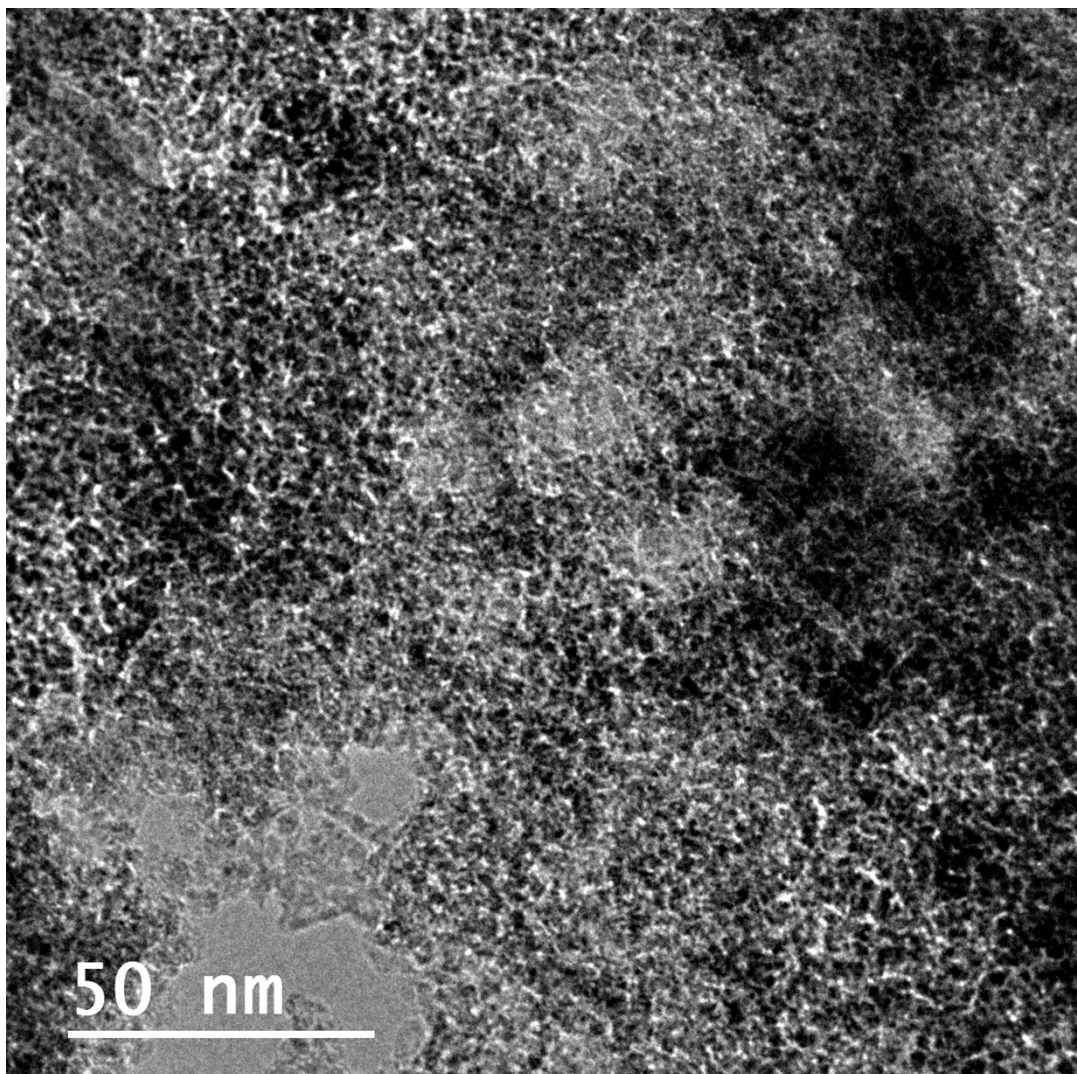


Fig. S4. TEM image of SiC-TM-1200-0.7 sample. SiC pore walls are composed of 2-10 nm crystallites.

Table S1. Parameters of powder XRD (022) peak for SiC-HS-0.6 series and por-SiC after thermal oxidation and HF wash treatments.

Sample	$\tau_1$ , nm	$\tau_2$ , nm	$S_1$ , %
SiC-HS-1200-0.6	25.9	1.97	10.6
SiC-HS-1300-0.6	20.3	2.03	13.1
SiC-HS-1400-0.6	27.3	2.28	14.9
SiC-1200-O2_HF	23.0	1.98	13.8
SiC-1300-O2_HF	23.9	2.03	20.6
SiC-1400-O2_HF	23.1	2.19	20.9

$\tau_1$  is the crystallite size of narrow Lorentzian peak component estimated by Scherrer equation;

$\tau_2$  is the crystallite size of wide Lorentzian peak component estimated by Scherrer equation;

$S_1$  is the area of narrow Lorentzian component related to overall peak area.

The size of large crystallites is independent on the pyrolysis temperature within the experimental error. The size of small crystallites demonstrates a slight growth with the PT increase. Fraction of the large crystallites which is determined by  $S_1$  parameter rises significantly with the PT as well after the oxidation/washing cycle. This fact demonstrates oxidation instability of small crystallites.

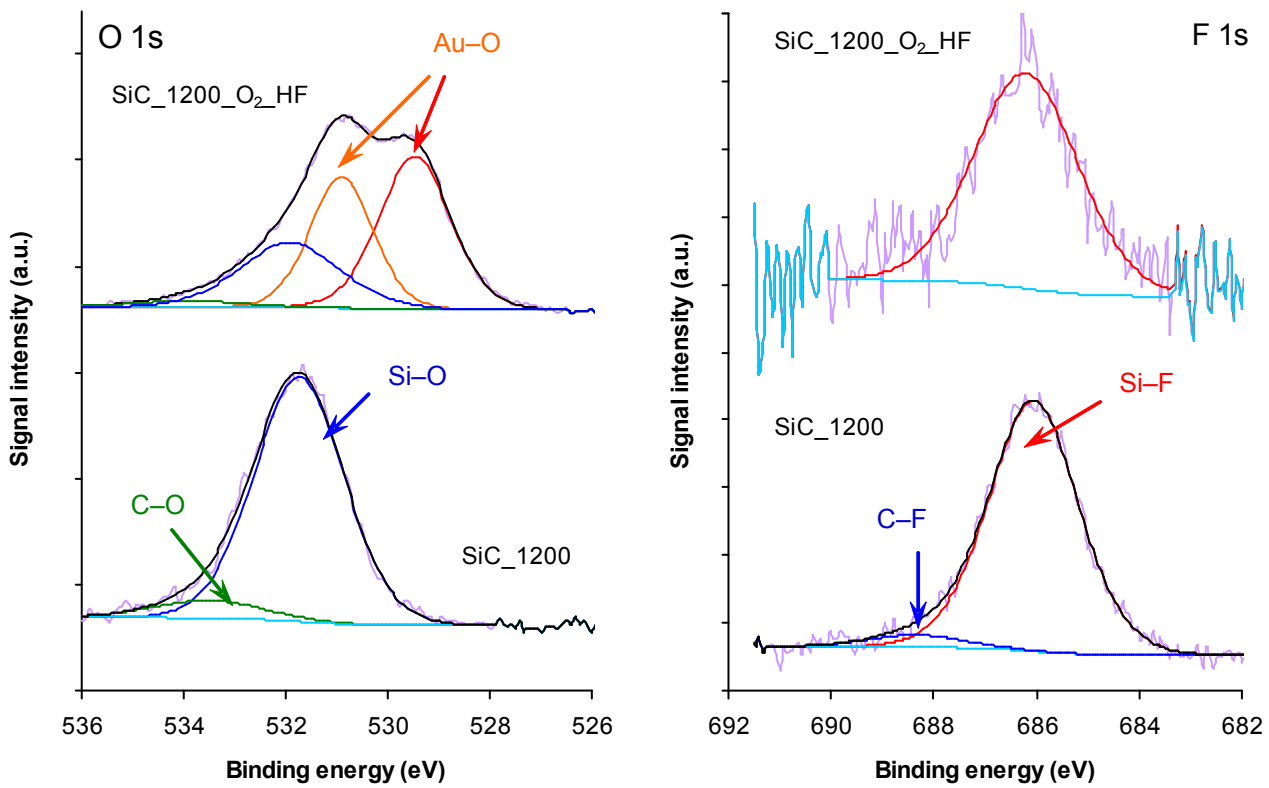


Fig. S5. XPS spectra (O 1s and F 1s) of SiC-HS-1200-0.6 and SiC-1200-O<sub>2</sub>\_HF samples.

The lines are presented mainly by Si–O (531.7 eV) and Si–F (686.0 eV) components. The components of O 1s line at 530.7 and 529.3 eV arise most probably due to the oxygen, chemisorbed on gold XPS support

Table S2. Chemical composition of SiC-HS-1200-0.6 and SiC-1200-O<sub>2</sub>\_HF samples derived from XPS (standard RSF values were used).

	Si	C	O	F
SiC-HS-1200-0.6	29.3	45.8	17.6	7.3
SiC-1200-O <sub>2</sub> _HF	43.6	49.1	6.1	1.1

Table S3. Textural characteristics of por-SiC obtained from 22 nm silica xerogel template, PCS: SiO<sub>2</sub>=0.7 by weight with addition of Ni(acac)<sub>2</sub>. The samples are indexed as SiC\_T\_X\_Ni, where T is the pyrolysis temperature, X is the initial Ni : PCS ratio (% wt.).

Sample	S <sub>BET</sub> , m <sup>2</sup> g <sup>-1</sup>	V <sub>pore</sub> , cm <sup>3</sup> g <sup>-1</sup>	D <sub>ads</sub> , nm	D <sub>des</sub> , nm	D <sub>BET</sub> , nm	h, nm	τ, nm
SiC_1200	438	0.97	22	13	9	2.8	4,6
SiC_1200_1.5Ni	396	0.96	25	18	10	3.1	7,0
SiC_1200_2.5Ni	313	0.97	31	22	12	4.0	9,4
SiC_1200_3.5Ni	288	0.98	41	24	14	4.3	10,7
SiC_1200_4.5Ni	270	0.92	51	30	14	4.6	15,3
SiC_1400	351	0.72	22	13	8	3.6	6,6
SiC_1400_1.5Ni	245	0.76	32	24	12	5.1	11,8
SiC_1400_2.5Ni	198	0.75	43	30	15	6.3	13,1
SiC_1400_3.5Ni	180	0.66	58	35	15	6.9	14,8
SiC_1400_4.5Ni	155	0.66	60	35	17	8.0	15,8
SiC_1300	426	0.89	22	11	8	2.9	-
SiC_1300_1.5Ni	338	0.93	22	15	11	3.7	-
SiC_1300_2.5Ni	300	0.91	29	20	12	4.2	-

S<sub>BET</sub> is the surface area; V<sub>s</sub> is the pore volume at p/p<sub>0</sub> = 0.98; D<sub>ads</sub> and D<sub>des</sub> are the maxima of pore size distributions from adsorption and desorption branches of the isotherm, respectively; D<sub>BET</sub> is the average pore size, calculated from the cylindrical pore model by formula 4V<sub>s</sub>/S<sub>BET</sub>, h = 4/(ρ<sub>SiC</sub>·S<sub>BET</sub>) is an average pore wall thickness in estimation of pore walls as the SiC cylinders, τ is the crystallite size, derived from Scherrer equation.

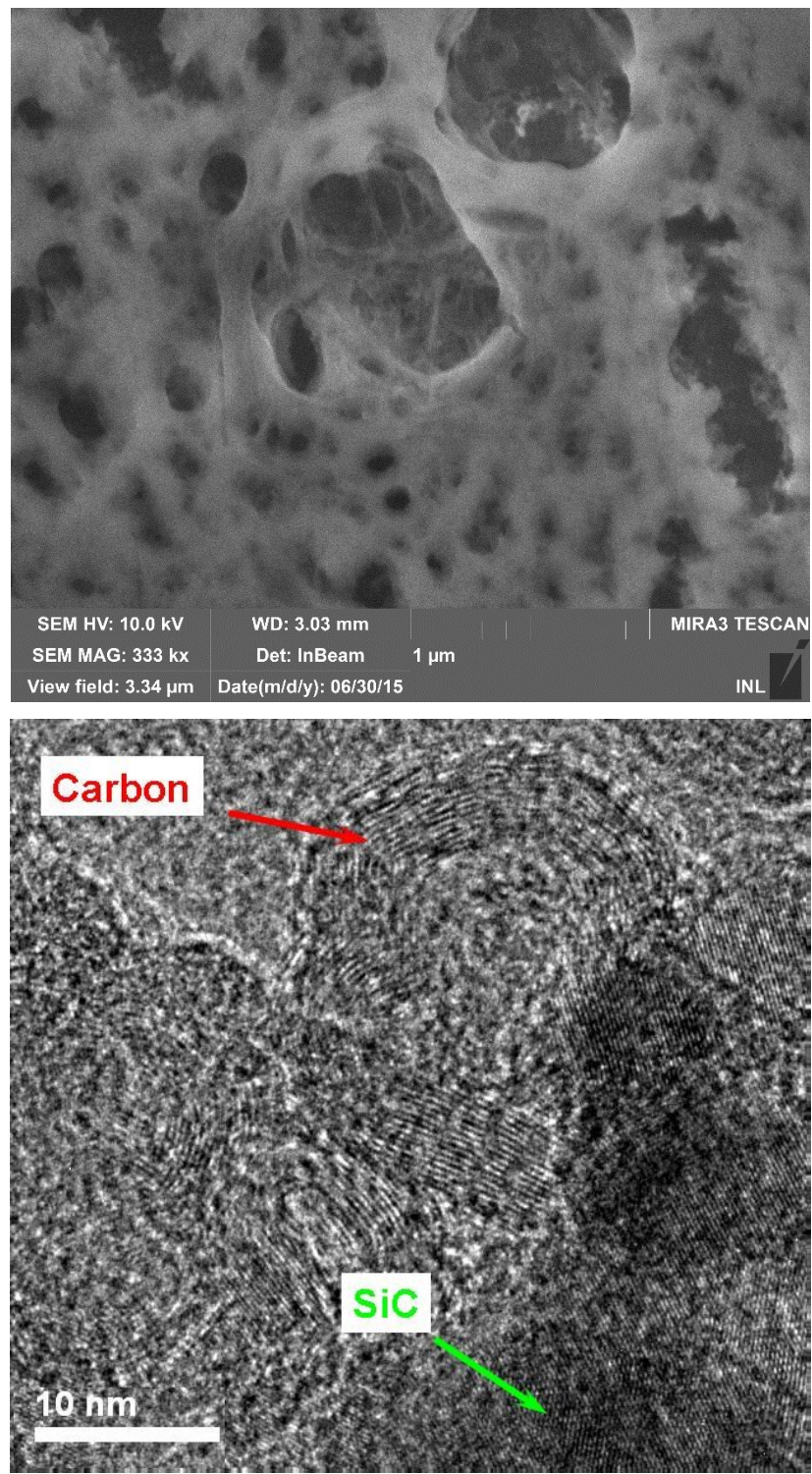


Fig. S6. SEM and HR-TEM images of SiC<sub>1200</sub>\_4.5Ni sample (see Table S2).